

Research Article

Optimization by Response Surface Methodology of Biodiesel Production from *Podocarpus falcatus* Oil as a Cameroonian Novel Nonedible Feedstock

Serges Bruno Lemoupi Ngomade ¹, Raoul Donald Tchuifon Tchuifon ²,
Rufis Fregue Tiegam Tagne ³, Meme Laloï Tongnang Ngueteu ¹,
Hugues Mahouli Patai ¹, George Ndifor-Angwafor Nche ¹,
and Solomon Gabche Anagho ¹

¹Research Unit of Noxious Chemistry and Environmental Engineering, Department of Chemistry, Faculty of Science, University of Dschang, Dschang, Cameroon

²Laboratory of Energy, Materials, Modeling and Method, Department of Process Engineering, National Higher Polytechnic School of Douala, University of Douala, Douala, Cameroon

³Department of Paper Sciences and Bioenergy, University Institute of Wood Technology, University of Yaoundé I, Mbalmayo, Cameroon

Correspondence should be addressed to George Ndifor-Angwafor Nche; nchegeorged4@yahoo.com and Solomon Gabche Anagho; sg_anagho@yahoo.com

Received 23 January 2022; Revised 5 March 2022; Accepted 18 March 2022; Published 4 April 2022

Academic Editor: Gonggang Liu

Copyright © 2022 Serges Bruno Lemoupi Ngomade et al. This is an open access article distributed under the Creative Commons Attribution License, which permits unrestricted use, distribution, and reproduction in any medium, provided the original work is properly cited.

The production of methyl esters (biodiesel) by the transesterification of *Podocarpus falcatus* oil (PFO) with methanol was optimized by response surface methodology (RSM) using the Box-Behnken design. The effects of parameters such as temperature, reaction time, and alcohol/oil molar ratio using yield and viscosity as responses were investigated. The optimum conditions for the production of biodiesel were as follows: temperature at 65°C, reaction time of 180 min, and molar ratio of 10:1, while the minimum viscosity was obtained for a temperature of 50°C, a reaction time of 120 min, and a molar ratio of 10:1. Physicochemical characterization by infrared spectroscopy (FT-IR) and UV visible spectroscopy showed that the free fatty acid (FFA) content of *Podocarpus* oil was 1.9%, which is less than the maximum of 2% recommended for the application of the one-step alkaline transesterification process. Also, the biodiesel obtained from the oil was seen to consist mainly of methyl esters, and that its physicochemical characteristics are within the standard set by the American Standard for Testing and Materials (ASTM).

1. Introduction

Despite its negative impact on the environment, the need for fossil fuels has increased due to population growth and rapid industrial development [1]. This situation has led to the search for alternative energy sources that could be sustainable and respectful of the environment [2]. Fossil fuels are one of the

most important energy sources, and they are widely used in various industries such as transport and thermal power plants, and their uses have caused serious pollution to the environment. Global crude oil demand in 2020 was estimated at 101.6 million barrels per day [3], while by 2040, aggregate energy demand will be around 30% higher than they were in 2010 [4], with a resultant increase in the emission of

greenhouse gases and the depletion of energy reserves. To remedy these problems, there has been the need to look for alternative energy sources.

Biodiesel, one of the main alternative fuels with low greenhouse gas emissions, is one of such alternatives. It is produced from various natural sources such as vegetable oils, animal fats, and algae [4, 5]. There are several methods for producing biodiesel from vegetable oils such as pyrolysis, dilution, microemulsion, and transesterification [6]. Among these methods, the transesterification process has been found to be more efficient and economical due to its easy implementation and relatively low cost [7]. During this process (Figure 1), three conversion reactions occur: the conversion of triglycerides to diglycerides, diglycerides to monoglycerides, and finally, the transformation of monoglycerides into glycerol. Each reaction uses one mole of alcohol in the presence of a catalyst, which could be acidic or basic, to chemically decompose the vegetable oil molecules into alkyl esters with glycerol as a by-product [8–10].

The transesterification process is governed by the control of several parameters that affect the desired product. It has become increasingly difficult and more expensive to control these parameters effectively by means of classical optimizations [11]. Current research is focusing on mathematical models obtained from experimental design to overcome this obstacle [10]. This method simultaneously studies the different factors that influence the process and their interactions with each other, while minimizing errors. The Box-Behnken (BB) design in response surface methodology (RSM) is generally used to optimize parameters influencing the transesterification reaction and using an appropriate software such as Statgraphics or STATISTICA [12].

The price of edible vegetable oils is relatively higher than that of diesel, and the use of these oils as a raw material for biodiesel production competes with food [13] and is not economical. Consequently, a solution is currently being sort through the use second generation raw materials such as inedible vegetable oils, used cooking oils, and animal fats. Thus, the use of inedible oils reduces the dependence on the use of edible vegetable oils for the production of biodiesel [14].

Podocarpus falcatus is an inedible oilseed species which belongs to the Podocarpaceae family. It grows at an altitude of 1,500–2,500 m above sea level in areas of average annual precipitation of 1,200–1,800 mm [15]. This inedible oleaginous plant is very abundant in Cameroon and can therefore be used as a raw material for the production of biodiesel. However, when we reviewed the literature, no work was reported on the production of biodiesel from *Podocarpus falcatus*. The novelty in the work is the search for the optimal conditions of the reaction of alkali-catalyzed transesterification (KOH) by response surface methodology to produce biodiesel. Another novelty is in the use of *Podocarpus falcatus* oil (PFO) as a new feedstock to produce biodiesel. The influence of process parameters such as temperature, methanol/oil molar ratio, and reaction time were investigated.

Different methods can be used to obtain PFO from its seeds, namely, the traditional extraction method, mechanical extraction, and chemical extraction [13]. Among these,

mechanical press methods are generally used to extract vegetable oils from oil plants with an oil content greater than 20% [13]. Generally, this process has the advantages of having a low production cost and the oil produced has low concentrations of free fatty acids [16]. Table 1 shows the fatty acid composition of PFO.

The challenge of our work lied in the in-depth application of the concepts of experiment methodology design, to study the parameters affecting the production of biodiesel derived from PFO, thus providing useful guidelines to promote the sustainable uses of biomass in general.

2. Material and Methods

2.1. Materials and Chemicals. All chemicals used such as methanol (99.9% purity), ethanol (98% purity), phenolphthalein, diethylether, sodium hydroxide (85% purity), and potassium hydroxide (85% purity) were purchased from Prolabo, Sion, Switzerland.

The fruits of *Podocarpus falcatus* were collected from the University of Dschang, Menoua Division in the West Region of Cameroon.

The freshly harvested fruits were stripped of their endocarps, dried in open air, and then shelled to obtain almond seeds. These almonds were further dried in the sun and then subjected to mechanical pressing extraction at the Renewable Energy Laboratory of the Faculty of Agricultural Sciences at the University of Dschang, Cameroon. About 300 g of raw materials was placed in a strong and perforated metal “cylindrical cage” and pressed by the movement of a piston. An iron tray was used in the cage to provide constant pressure through the volume of material and to speed up the oil extraction process. The compressed almonds were evacuated through a circular opening located at the bottom of the cage. The yield of the extracted oil was determined by the formula used by Carr [16].

$$\text{Yield (\%)} = \frac{\text{mass of oil extracted (g)}}{\text{mass of sample (g)}} \times 100. \quad (1)$$

Figure 2 gives the different forms of biomass used and the oil obtained.

2.2. Biodiesel Production. Biodiesel was synthesized according to the procedure reported by Hassan and Fadhil [17]. The transesterification process was performed in a 100 mL three-necked round bottom flask. 50 g of oil was used in each of the 15 experiments. For each experiment, the oil was carefully transferred to the flask and preheated on a hotplate to its reaction temperature. A solution of potassium methoxide was freshly prepared and added to the preheated oil, and the mixture was heated to reflux and stirred. After the transesterification process, the mixture underwent separation in a separating funnel for six hours. The upper phase containing the biodiesel was washed several times with hot water to remove residual impurities. After washing, the biodiesel phase was dried in an oven at a temperature of 110°C for four hours to evaporate

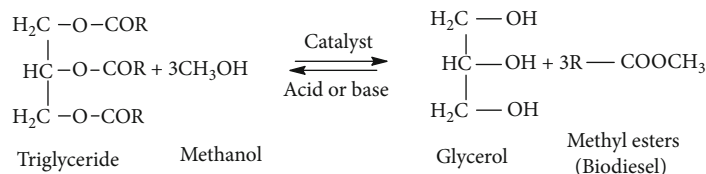


FIGURE 1: General equation of the transesterification reaction.

TABLE 1: Fatty acid composition of *Podocarpus falcatus* oil [15].

| Fatty acids | Content (%) | Saturation level |
|-----------------------|-------------|------------------|
| Palmitic acid (16:0) | 8.87 | Saturated |
| Stearic acid (18:0) | 4.45 | Saturated |
| Oleic acid (18:1) | 78.94 | Monounsaturated |
| Linoleic acid (18:2) | 4.70 | Polyunsaturated |
| Linolenic acid (18:3) | 3.04 | Polyunsaturated |

the traces of water and methanol. The methodology steps are illustrated in Figure 3.

The yield of the biodiesel from the esterification reaction was calculated according to the following equation:

$$\text{Yield (\%)} = \frac{\text{mass of biodiesel produced (g)}}{\text{mass of oil used (g)}} \times 100. \quad (2)$$

2.3. Experimental Design. Three-factor design was applied with a total of 15 experimental runs generated by the BB design. The parameters selected for optimization were as follows: methanol/oil molar ratio, A; reaction time (min), B; and temperature ($^{\circ}\text{C}$), C. Table 2 shows the 15 experimental runs generated. The reactions were carried out at various alcohol/oil molar ratios (6:1–10:1), reaction times (60 min–180 min), and at temperatures (50–80 $^{\circ}\text{C}$). Potassium hydroxide (KOH: 1 wt.%) was used as a catalyst for all the transesterification reactions. The parameter ranges were selected on the basis of a review of the literature [18, 19].

2.4. Statistical Analysis. The data obtained from the experiments were analysed using the STATGRAPHIC 16 software, and the response surfaces were plotted from version 8 of the STATISTICA software. The BB design reduces the number of experiments without loss of precision and more efficiently assesses complex response functions compared to other designs [20–22]. The number of experimental trials is estimated by equation (3).

$$N = k^2 + k + C_p = 3^2 + 3 + 3 = 15, \quad (3)$$

where k and C_p are the number of variables studied and the number of points replicated, respectively [23]. Table 3 presents the parameters of independent variables using the BB design.

The effect of the variables (x_1 , x_2 , and x_3) on the viscosity and the yield of the product was evaluated using a second order polynomial model given by equation (4) [24].

$$Y = a_0 + \sum_{i=1}^k a_i x_i + \sum_{i=1}^k a_{ii} x_i^2 + \sum_{i=1}^k \sum_{j=1}^k a_{ij} x_i x_j + \varepsilon, \quad (4)$$

where Y is the response obtained, a_0 is a constant, a_i is the linear effect of the input factor x_i , a_{ij} defines a linear interaction between the factors x_i and x_j , a_{ii} is the quadratic effect of the factor x_i , and ε is random error. The goodness of the fit of the model was assessed using a test of significance and analysis of variance (ANOVA).

The empirical model obtained was validated using the STATGRAPHIC 16 software as an evaluation instrument. The model is considered good when the experimental values obtained are close to those predicted by the t -test and the p value. In general, a model is validated when R^2 is greater than 75% or the p value $\leq 5\%$, with a confidence level of 95% [25].

2.5. Physicochemical Characterizations

2.5.1. Fourier Transform Infrared Spectrometry (FT-IR) Analysis. The functional groups of the extracted oil and the produced biodiesel were determined by FT-IR spectroscopy using the Thermo Scientific Nicolet iS5 FT-IR spectrometer. A few drops of each sample of biodiesel and oil were placed in the previously cleaned sample compartment and scanned using an IR spectrum of a wavelength range of 4,000–500 cm^{-1} , using the OMNIC Spectra software.

2.5.2. UV Spectroscopy Analysis. In order to study changes in electronic energy levels, π electron systems, and conjugate unsaturation within molecules present in *Podocarpus falcatus* oil and biodiesel, a Thermo Scientific UV/Vis spectrophotometer, GENESYS 10S was used. The spectra scans were 200–600 nm, with a 1 cm quartz cuvette. All samples were diluted in ethanol.

2.5.3. Physicochemical Properties of the Oil and Biodiesel Produced. The objective of this characterization was to determine the physicochemical properties of the extracted oil and the produced biodiesel in order to compare them with European (EN 14214) and American (ASTM D6751) standards. These parameters were as follows: acid number, saponification number, iodine number, cetane number, calorific value, pour point, density, and viscosity. The reproducibility of all the measurements was verified by repeating two experiments under the same conditions.



FIGURE 2: Different forms of *Podocarpus falcatus* fruit and *Podocarpus* oil: (a) fresh fruits; (b) seeds before peeling; (c) seeds after peeling; (d) *P. falcatus* oil.

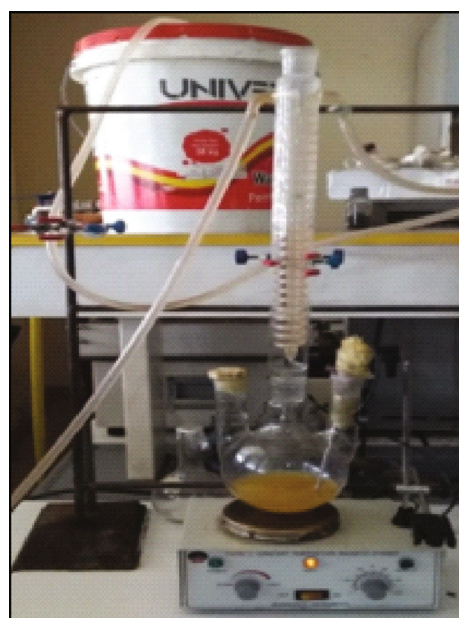
2.5.4. Determination of the Acid and the Free Fatty Acid Levels. The acid level of the oil and of the biodiesel was determined according to the protocol derived from the AFNOR NF EN ISO660 standard of 2009. Briefly, 1.5 g of sample was placed in a 250 mL Erlenmeyer flask and then supplemented with 50 mL of a 1:1 (v:v) neutralized solution of ethanol and diethyl ether. The mixture was titrated with an ethanolic solution of potassium hydroxide KOH (0.1 N) until the appearance of a persistent pink colour. The values of the acid number (I_A) and the free fatty acid number (I_{FFA}) were calculated using the formulas in equations (5) and (6):

$$I_A = \frac{N \times V \times 56.1}{m}, \quad (5)$$

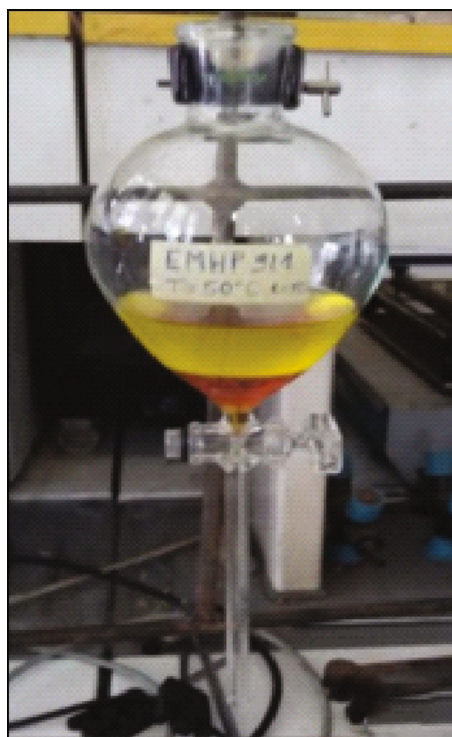
$$I_{\text{FFA}} = \frac{I_A}{1.99}. \quad (6)$$

N is the normality of the ethanolic solution of KOH in eq/L; V is the volume of the ethanolic KOH solution used for the titration in mL; m is the mass of the test sample in grams.

2.5.5. Determination of the Saponification Index. The saponification indices of the oil and the biodiesel were determined according to the protocol derived from the AFNOR NFT60-206 standard. Briefly, 1.5 g of fatty substance was placed in a flask, followed by the addition of 20 mL of alcoholic potassium hydroxide solution (0.5 N). The mixture was heated at reflux in a water bath for 45 minutes until complete saponification. After cooling, the excess KOH was titrated with a solution of hydrochloric acid, HCl (0.5 N) in the presence of phenolphthalein, until the pink colour of the solution turned colourless. A blank test was carried out beforehand under the same conditions, by titrating the ethanolic solution of KOH in the absence of fatty substances.



(a)



(b)



(c)

FIGURE 3: Steps of (a) reaction, (b) settling, and (c) washing the biodiesel.

TABLE 2: Experimental matrix and theoretical experiments and responses.

| Test | Temperature (°C) | Time (min) | Molar ratio | Viscosity (mm ² /s) | | Yield (%) | |
|------|------------------|------------|-------------|--------------------------------|---------|-----------|---------|
| | (x_1) | (x_2) | (x_3) | Y_V | Y_V^* | Y_R | Y_R^* |
| 1 | 65.0 | 60.0 | 10.0 | 3.84 | 3.945 | 83.6 | 83.9725 |
| 2 | 65.0 | 120.0 | 8.0 | 4 | 4.12 | 96.1 | 95.2533 |
| 3 | 65.0 | 180.0 | 10.0 | 3.84 | 3.715 | 94.3 | 93.7875 |
| 4 | 65.0 | 180.0 | 6.0 | 4.64 | 4.765 | 87.12 | 86.7475 |
| 5 | 80.0 | 120.0 | 10.0 | 4.10 | 4.02 | 88.66 | 89.7725 |
| 6 | 65.0 | 120.0 | 8.0 | 4.08 | 4.12 | 95.40 | 95.2533 |
| 7 | 80.0 | 60.0 | 8.0 | 4.08 | 4.285 | 93.46 | 91.975 |
| 8 | 80.0 | 180.0 | 8.0 | 4.74 | 4.715 | 87.9 | 87.3 |
| 9 | 50.0 | 60.0 | 8.0 | 4.42 | 4.445 | 85.86 | 86.46 |
| 10 | 50.0 | 120.0 | 10.0 | 3.58 | 3.68 | 94.72 | 92.7475 |
| 11 | 80.0 | 120.0 | 6.0 | 5.54 | 5.54 | 91.22 | 92.1925 |
| 12 | 65.0 | 60.0 | 6.0 | 5.64 | 5.54 | 90.88 | 91.3925 |
| 13 | 50.0 | 120.0 | 6.0 | 4.72 | 4.8 | 92.82 | 91.7075 |
| 14 | 50.0 | 180.0 | 8.0 | 3.78 | 3.575 | 94.82 | 96.305 |
| 15 | 65.0 | 120.0 | 8.0 | 4.28 | 4.12 | 94.26 | 95.2533 |

x_1 : reaction temperature; x_2 : reaction time; x_3 : alcohol/oil molar ratio; Y_V : experimental viscosity; Y_V^* : theoretical viscosity; Y_R : experimental yield; Y_R^* : theoretical yield.

TABLE 3: Parameter of independent variables used by the BB plan for the optimization of oil transesterification of the oil *Podocarpus falcatus*.

| Variables | Symbols | Level | | |
|---------------------|---------|-------|-----|------|
| | | -1 | 0 | 1 |
| Temperature (°C) | A | 50 | 65 | 80 |
| Reaction time (min) | B | 60 | 120 | 180 |
| Molar ratio | C | 6:1 | 8:1 | 10:1 |

The saponification index was calculated by formula (7):

$$I_S = \frac{V_0 - V}{m} \times N \times 56.1. \quad (7)$$

V_0 is the volume of HCl (mL) required to titrate the blank; V is the volume of HCl (mL) necessary to titrate the sample to be analysed; N is the normality of HCl (eq/L); m is the sample mass in grams for the test.

2.5.6. Determination of the Iodine Value. The AFNOR NFT60-203 standard was used to determine the iodine numbers of oil and biodiesel according to the following protocol: 1g of sample was introduced into a 250 mL Erlenmeyer flask, followed by addition of 15 mL of carbon tetrachloride and 25 mL of Wijs reagent. The mixture was stoppered, stirred, and left in the dark for one hour. Then, 20 mL of 10% potassium iodide (KI) and 150 mL of distilled water were added to the mixture, and the excess iodine was titrated with a sodium thiosulfate $\text{Na}_2\text{S}_2\text{O}_3$ solution (0.1 N) using starch solution as an indicator. Equivalence point was identified by the change in colour from a blue-violet solution to colourless. A blank test was carried out in the same way.

The iodine number was calculated by the following formula:

$$I_I = \frac{V_0 - V}{m} \times 126.9 \times N, \quad (8)$$

where V_0 is the volume of sodium thiosulfate $\text{Na}_2\text{S}_2\text{O}_3$ (0.1 N) required to titrate in the blank test, V is the volume (in mL) of sodium thiosulfate $\text{Na}_2\text{S}_2\text{O}_3$ (0.1 N) necessary to titrate the sample, m is the test sample mass (in g), and N is the normality in eq/L of $\text{Na}_2\text{S}_2\text{O}_3$.

2.6. Determination of the Cetane Number. Biodiesel cetane number (CN) was calculated by the correlation given by Krisnangkura [26] relating the iodine number (I_I) and the saponification index (I_S), as shown by equation (9):

$$\text{CN} = 46.3 + \frac{5458}{I_S} - 0.225 I_I. \quad (9)$$

2.6.1. Determination of the Calorific Value. The calorific value (P_C) of biodiesel was calculated from the model developed by Demirbas [27] using the iodine number (I_I) and the saponification number (I_S) as illustrated by equation (10):

$$P_C = 49.43 - (0.015 I_I) - (0.041 I_S). \quad (10)$$

2.6.2. Density Determination. The density of a substance is defined as the mass of that substance contained in a fixed volume, under the same well-defined temperature and pressure conditions [28]. The respective masses of the oil and biodiesel corresponding to well-defined volume were measured using a Sartorius balance. Knowledge of these masses

and volumes was used to determine the density and relative density according to equations (11) and (12):

$$\rho = \frac{m}{V}, \quad (11)$$

$$d = \frac{\rho}{\rho_e}. \quad (12)$$

m is the mass of the sample in grams (g); V is the volume of the sample in millilitres (mL); ρ is the density of the sample in grams per liter (g/L); ρ_e is the density of water (g/L).

2.6.3. Viscosity Measurement. The kinematic viscosity was studied in accordance with standard ASTM 445, using a capillary viscometer of the UBBELOHDE type, a viscometer support allowing the instrument to be kept in a vertical position, a bath equipped with a thermostat, a stopwatch to measure time, and a filter paper. For a given test temperature, the viscosity was determined by the formula given by equation (13):

$$\eta = k * t, \quad (13)$$

where k is viscometer constant, t is the liquid flow time in seconds, and η is viscosity in mm^2/s .

3. Results and Discussion

3.1. Optimization by Response Surface Methodology. Several parameters influence the transesterification reaction, the most important of which are the temperature (x_1), the reaction time (x_2), and the methanol/oils molar ratio (x_3). The regression surface equations and response curves were obtained as a function of these three parameters.

3.1.1. Regression Equation for Methyl Esters and Viscosity. In order to study the effects of the interaction between the parameters affecting the transesterification reaction on the response variables, yield, and viscosity, experiments were carried out by varying these parameters and using the BB design. The experimental results were fitted to the polynomial equations for viscosity and methyl ester (biodiesel) yield, which are presented in equations (14) and (15):

$$\begin{aligned} Y_{\text{methyl ester}} = & 11.0006 + 1.10835 * x_1 + 0.280403 * x_2 \\ & + 7.9725 * x_3 - 0.00296296 * x_1 * x_1 \\ & - 0.00403333 * x_1 * x_2 - 0.0371667 * x_1 * x_3 \\ & - 0.00102685 * x_2 * x_2 + 0.031375 * x_2 * x_3 \\ & - 0.587917 * x_3 * x_3, \end{aligned} \quad (14)$$

$$\begin{aligned} Y_{\text{viscosity}} = & 14.1944 - 0.0325185 * x_1 - 0.0419167 * x_2 \\ & - 1.39667 * x_3 + 0.000196296 * x_1 * x_1 \\ & + 0.000361111 * x_1 * x_2 - 0.0025 * x_1 * x_3 \end{aligned}$$

$$\begin{aligned} & + 0.00000671296 * x_2 * x_2 + 0.001875 * x_2 * x_3 \\ & + 0.0635417 * x_3 * x_3. \end{aligned} \quad (15)$$

In the above equations, a positive sign in front of the terms indicates a synergistic effect while a negative sign indicates an antagonistic effect. Therefore, temperature (x_1), reaction time (x_2), molar ratio (x_3), temperature-molar ratio (x_1x_3), and time-molar ratio (x_2x_3) interactions played an important role in increasing the yield, while the temperature-time (x_1x_2) interactions and the quadratic temperature-temperature (x_1x_1), time-time (x_2x_2), and molar-molar ratio (x_3x_3) effects had a negative contribution to the yield of the biodiesel. In addition, the effects of temperature-time (x_1x_2), time-molar ratio (x_2x_3) interactions, quadratic temperature-temperature (x_1x_1), and molar-molar ratio (x_3x_3) increased the viscosity. Also, the temperature (x_1), the reaction time (x_2), the molar ratio (x_3), and the temperature-molar ratio interaction (x_1x_3) promoted the decrease in viscosity.

3.1.2. Analysis of Model Variance. The validation of the model was made with the coefficient of determination R^2 , which was 0.95 for the viscosity and 0.94 for the yield, thus indicating that this model conformed with the experimental results. Linear, quadratic, or interaction effects of variables on responses were investigated using ANOVA. With regard to Table 4, it can be seen that the variables which had a more significant effect on the yield of biodiesel were the interactions between temperature and the methanol/oil ratio and between temperature and time where $p < 0.05$, followed by the quadratic terms of reaction time and molar ratio, which also had $p < 0.05$. We also note that the alcohol/oil molar ratio had a more significant effect on the viscosity ($p < 0.05$), followed by the reaction temperature and the interaction between temperature and reaction time.

3.1.3. Study of the Effects of Factors on Viscosity. The variation in the viscosity of biodiesel as a function of the interaction between reaction time and temperature is illustrated by the 3D response surface curve, coupled to the contour diagram, in Figure 4(a). This figure shows that the reaction time is a factor that changes in the opposite direction to that of the change in kinematic viscosity. When moving from low values for the reaction time to high values (60 min and 180 min), we saw that the viscosity decreased significantly from 5.54 mm^2/s to 3.78 mm^2/s . Since transesterification is a reaction which greatly reduces the viscosity of oils, the high viscosity observed at low reaction times could be due to incomplete conversion of oil to methyl ester. Unreacted oil could thus increase the viscosity of the biodiesel [29]. Furthermore, the high viscosity observed after the optimum reaction time could be attributed to side reactions, such as saponification and esterification, since the reaction is reversible and takes place in an alkaline medium. These phenomena can lead to difficulties in separating the biodiesel layer from glycerol [30]. These observations were similar to those made by Chigozie et al. [31]. According to the American material standard test (ASTM D9751), the standard viscosity

TABLE 4: ANOVA results for biodiesel yield and viscosity.

| Source | Sum of squares | Viscosity | | | Yield | | |
|-----------------------|----------------|-----------------------|---------|---------|----------------|--------------------------------------|---------|
| | | Df | F-ratio | p | Sum of squares | F-ratio | p |
| x_1 (temperature) | 0.4802 | 1 | 10.73 | 0.0220* | 6.09005 | 2.33 | 0.1878 |
| x_2 (reaction time) | 0.0968 | 1 | 2.16 | 0.2012 | 14.9605 | 5.71 | 0.0624 |
| x_3 (molar ratio) | 3.2258 | 1 | 72.11 | 0.0004* | 0.2312 | 0.09 | 0.7783 |
| x_1^2 | 0.0072 | 1 | 0.16 | 0.7048 | 3.20493 | 0.63 | 0.4645 |
| x_1x_2 | 0.4225 | 1 | 9.44 | 0.0277* | 52.7076 | 20.13 | 0.0065* |
| x_1x_3 | 0.0225 | 1 | 0.50 | 0.5099 | 4.9729 | 1.90 | 0.2267 |
| x_2^2 | 0.0022 | 1 | 4.53 | 0.8349 | 50.4567 | 19.27 | 0.0071* |
| x_2x_3 | 0.2025 | 1 | 4.53 | 0.0867 | 56.7009 | 21.65 | 0.0056* |
| x_3^2 | 0.2385 | 1 | 5.33 | 0.0690 | 20.4197 | 7.80 | 0.0383* |
| Total error | 0.2237 | 5 | | | 13.0942 | | |
| $R^2 = 0.95449$ | | R^2 adjusted = 0.87 | | | | $R^2 = 0.94$; R^2 adjusted = 0.83 | |

*Significant at 95% confidence interval.

of conventional diesel is around 1.9-2.6 mm²/s. Therefore, a viscosity value outside this range does not have the properties that can be adapted to a diesel engine [32].

Figure 4(b) further shows that the methanol/oil molar ratio did not have a significant effect on viscosity. This was also confirmed by the low value of the constant observed compared to the molar ratio factor (x_3) in equation (15). This is not surprising, since after the reaction, the biodiesel was completely separated from the glycerol.

3.1.4. Study of the Effects of Methanol/Oil Molar Ratio, Reaction Time, and Temperature on the Biodiesel Yield. To investigate the interaction effects of the parameters on the reaction yield, two 3D response curves were plotted as shown in Figures 5(a) and 5(b) obtained using RSM. Figure 5(a) shows the interaction effect of reaction time and molar ratio on biodiesel yield. With respect to this figure, we noticed that high yields of 96.1% were obtained at relatively long reaction times of 120-180 min and molar ratios of 10:1 when the temperature was fixed at its average value of 50°C. This high yield of methyl ester could be due to the fact that the methanolysis of PFO is a reversible reaction and depends on the stoichiometry of the reaction. Indeed, an excess of alcohol in a molar ratio range 6:1 to 10:1 is needed to push the equilibrium in the direction of methyl ester production [33]. Moreover, for a very short reaction time (60 min), the low yields recorded could be explained by incomplete reactions. The optimal reaction time (180 min) being the longest duration could be linked to the moderate temperature, 50°C. It can be noticed that the interaction effect between reaction time and molar ratio has a positive effect on the reaction yield, as shown in equation (14). According to the results shown in Figure 5(b), the highest biodiesel yield (96.1%) was observed at the moderate reaction temperature (50°C) when the molar ratio was set at a value of 10:1. A slight reduction in yield was observed at temperature above 60°C, due to saponification reaction, which is faster than transesterification at high temperature

[34, 35]. Fadhil [32] obtained a similar result where he had an optimum production of esters from *Prunus amygdalus* seed oil at an optimum reaction temperature of 50°C.

The study of the effects of the various parameters and their reciprocal interactions led to the determination of the optimal conditions mentioned in Table 5:

3.2. Yield of Oil and Biodiesel Produced. *Podocarpus* oil was obtained with a yield of 47.8%; this may be because we used the power press. Moreover, the biodiesel produced under optimal conditions resulted in a yield of 96.1% (Figure 6). This value was very close to that predicted by the BB plan used.

3.3. Physicochemical Characteristics of Oil and Biodiesel. The physicochemical properties of biodiesel produced from PFO under optimum reaction conditions were measured according to ASTM standards. These properties were compared with those of PFO and diesel as shown in Table 6. From the results presented in this table, it can be seen that the calorific value of biodiesel produced from PFO is lower than that of diesel. This may be due to the higher oxygen content of biodiesel compared to diesel. Indeed, it has been demonstrated by Yamane et al. [36] that the presence of oxygen in the fuel improves combustion properties and emissions but lowers the calorific value. From the results presented in Table 6, it is clear that biodiesel has a lower density than PFO. This lower density of biodiesel compared to PFO is linked to the formation of methyl esters by eliminating glycerol. These results are close to those found by Tchuifon et al. [37].

Viscosity is an important parameter that affects fuel injection, lubrication, and atomization [38]. Fuels of high viscosity tend to form deposits in the engine. However, Table 6 shows that the kinematic viscosity of PFO decreased from 29.53 to 3.58 mm²/s at 40°C. This significant drop in viscosity confirms the efficiency of the transesterification reaction. Moreover, it is important to note that the high

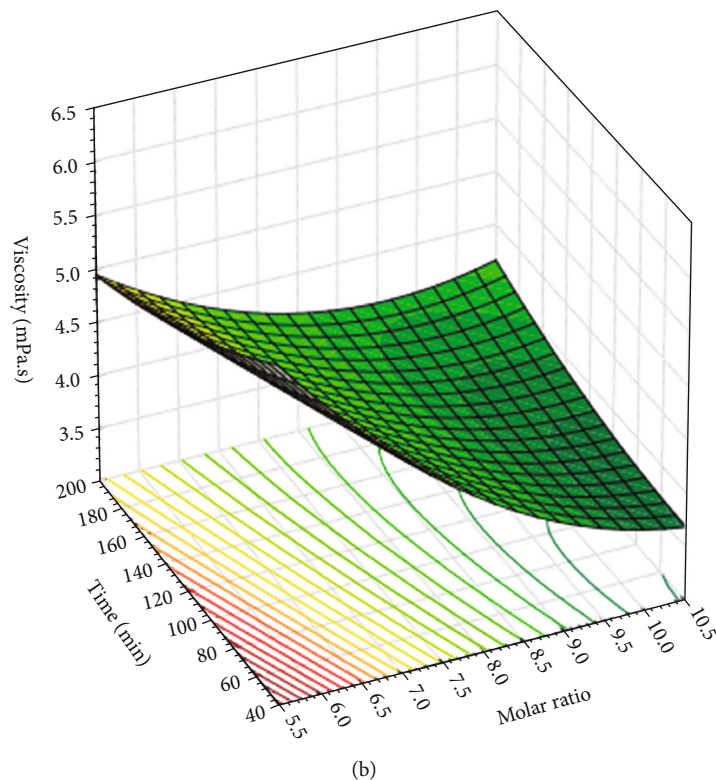
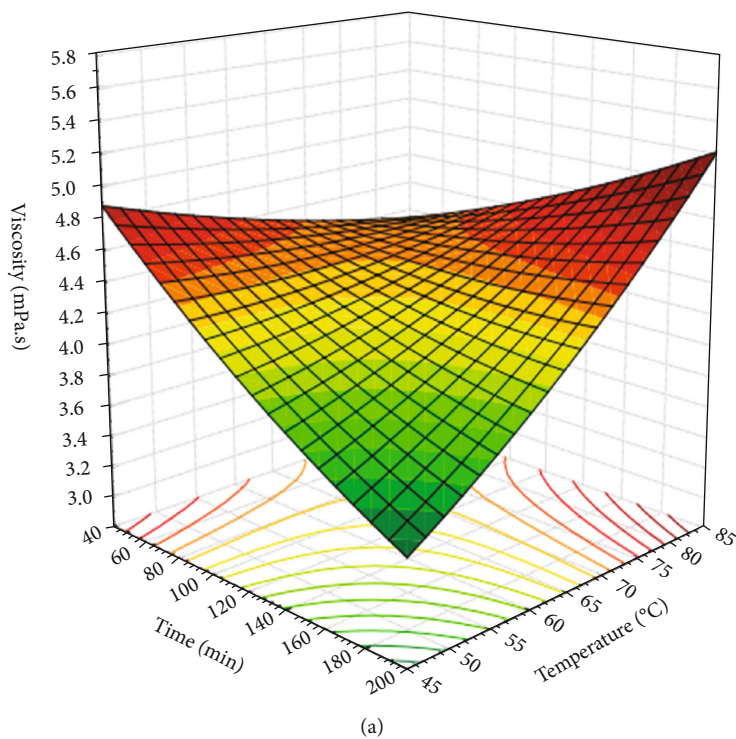
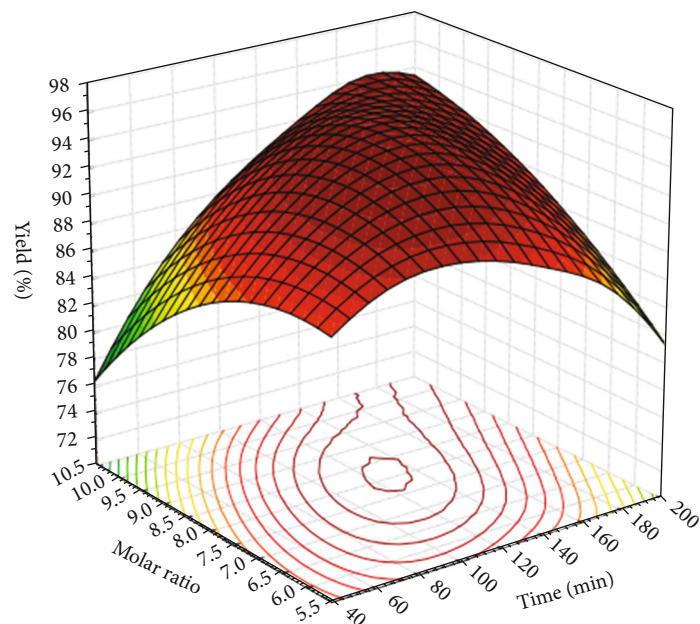


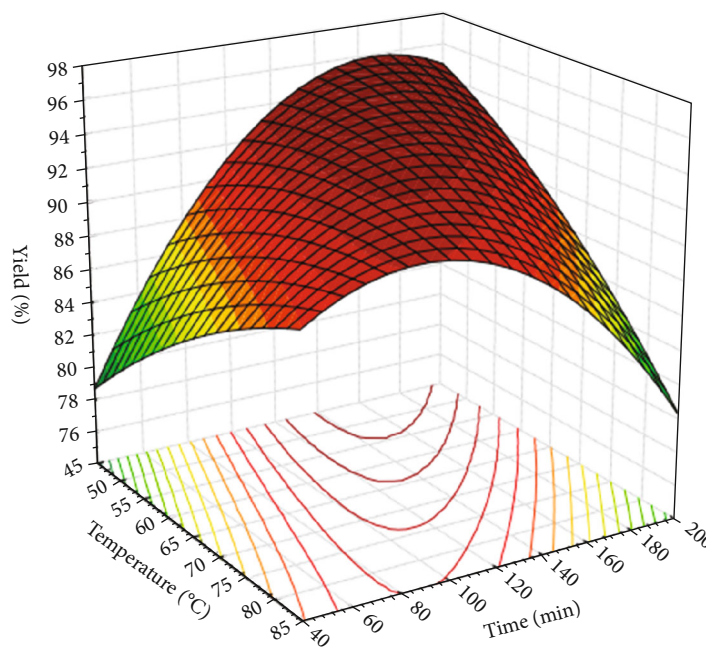
FIGURE 4: (a) Response surface contour for the effect of interaction between temperature and time on viscosity (KOH concentration: 1 wt.%). (b) Response surface contour for the effect of the interaction between time and molar ratio on viscosity (KOH concentration: 1 wt.%).

initial viscosity of this oil is due to its higher molecular weight compared to that of diesel fuel [39]. The interesting information is that the kinematic viscosity of biodiesel produced from *Podocarpus falcatus* oil is in the range 1.9-6.0 mm²/s as specified by ASTM. When a biodiesel having

a viscosity in this range is used in a diesel engine, it helps to lubricate parts of the engine [40]. Pour point analysis in the characterization of biodiesel is very important because it determines the suitability of the biofuel for large-scale storage. Pour point is the lowest temperature at which the



(a)



(b)

FIGURE 5: (a) Response surface contour for the effect of the interaction between time and molar ratio on yield (KOH concentration: 1 wt.%). (b) Response surface contour for the effect of the interaction between time and temperature on yield (KOH concentration: 1 wt.%).

TABLE 5: Optimal viscosity and yield conditions.

| Parameters | Optimal values of parameters | | Predicted responses | |
|---------------------|------------------------------|-----------|---------------------------|---------|
| | Viscosity | Yield | Viscosity | Yield |
| Temperature (°C) | 79.985 | 50 | | |
| Reaction time (min) | 60.0 | 180 | 5.4738 mm ² /s | 98.738% |
| Molar ratio | 6.00027/1 | 9.99997/1 | | |

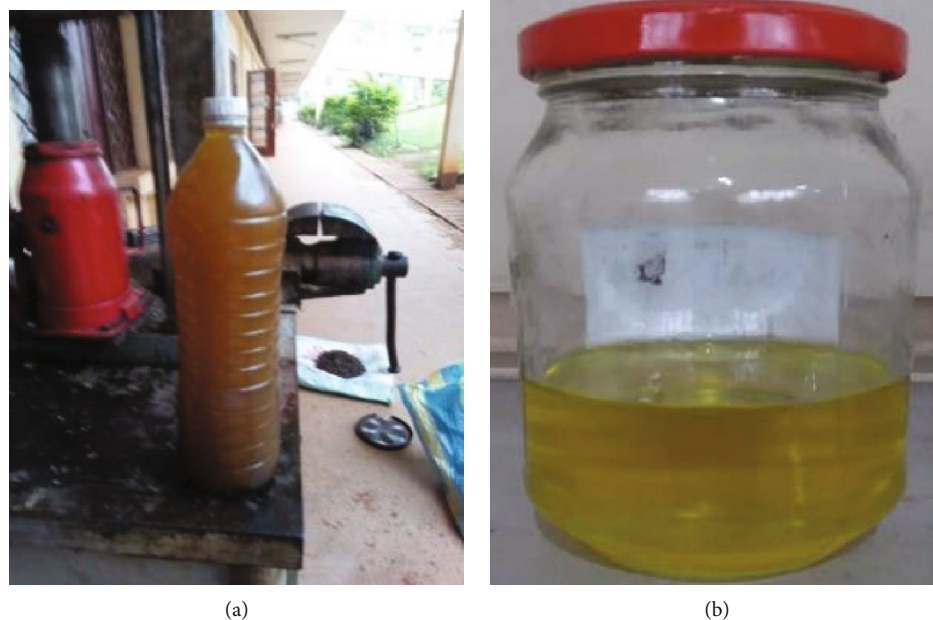


FIGURE 6: (a) *Podocarpus falcatus* oil. (b) Optimized biodiesel.

TABLE 6: Physicochemical properties of PFO and biodiesel compared to ASTM D6751.

| Properties | Units | PFO | Biodiesel | Diesel | ASTM D6751 |
|----------------------|-------------------------|--------|-----------|--------|------------|
| Density (at 15°C) | kg/m ³ | 922 | 872 | 845 | 880 |
| Viscosity (40°C) | mm ² /s | 29.53 | 3.58 | 2.4 | 1.9-6 |
| Pour point | °C | -8.6 | -15.20 | -17 | -15 at -16 |
| Calorific value | MJ/kg | 39.47 | 39.87 | 42.54 | 35 |
| Cetane number | - | 42.06 | 51.03 | 50 | 48-60 |
| Acid index | mg KOH/g | 1.90 | 0.40 | - | Max. 0.5 |
| Iodine number | g I ₂ /100 g | 147.10 | 103.10 | - | - |
| Saponification index | mg KOH/g | 189.11 | 195.44 | - | - |

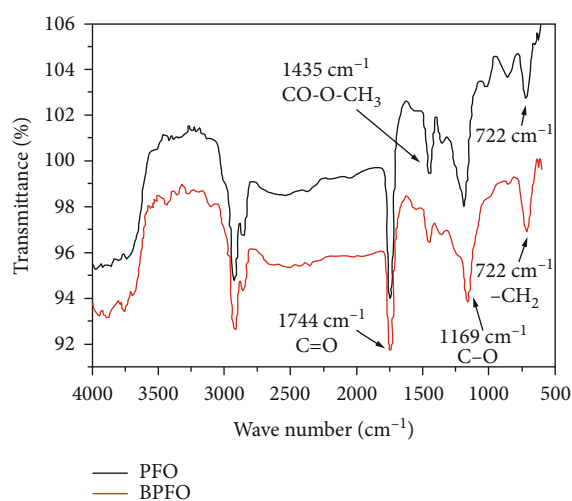


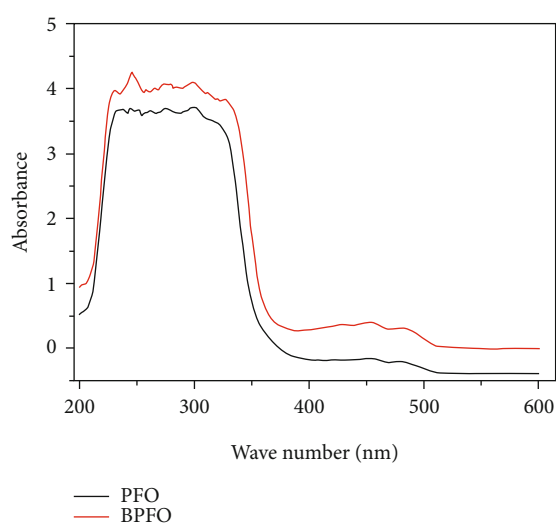
FIGURE 7: FT-IR spectra of *Podocarpus falcatus* oil (PFO) and biodiesel (BPFO).

fuel can still flow before it has gelled. This also reflects the biodiesel's ability to be used in cold climates [41]. The pour point found in this work is -15°C for the biodiesel obtained. On the other hand, the pour point value of -8.6°C obtained for *Podocarpus falcatus* oil is significantly higher than that of biodiesel. This could be due to the presence of glycerol in this oil which makes the medium more viscous and thus promotes gelation. This result is in harmony with that found by Fadhil et al. [42]. The cetane number (CN) of PFO (42.06) is lower than that of biodiesel (51.03). This variation can be attributed to the unsaturated fatty acids present in the oil. Chemical properties such as acid value, saponification value, and iodine value of PFO and biodiesel were determined and compared in Table 6. It appears that these properties are comparable with the standards of the American Society for the Testing of Materials (ASTM).

3.4. Analysis by IR-TF Spectrometry of Oil and Biodiesel. Figure 7 shows the superimposed infrared spectra of *Podocarpus falcatus* oil and the biodiesel obtained from it.

TABLE 7: Main position of characteristic bands for oil and biodiesel.

| PFO | Functional groups | Absorption vibration (cm^{-1}) | BPFO | Functional groups |
|------|---|---|------|---|
| 722 | Deformation $-\text{CH}_2$ | 722 | 722 | Tilting $-\text{CH}_2$ |
| 1362 | CH_2 group deformation vibration | 1362 | 1362 | CH_2 group deformation vibration |
| 1744 | Elongation $\text{C}=\text{O}$ | 1742 | 1742 | Elongation $\text{C}=\text{O}$ |
| 1169 | Stretching $\text{C}-\text{O}$ | 1194 | 1194 | Elongation $\text{C}-\text{O}$ |
| | | 1171 | 1171 | Elongation |
| | | 1110 | 1110 | $\text{C}-\text{O}-\text{O}-\text{CH}_2-\text{C}$ |
| 1435 | Deformation vibration CH_2 | 1435 | 1435 | Methyl ester group ($\text{CO}-\text{O}-\text{CH}_3$) |
| 2925 | Elongation $-\text{CH}_2$ | 2927 | 2927 | Elongation $-\text{CH}_2$ |

FIGURE 8: Superimposed UV-VIS spectra of *Podocarpus falcatus* oil (PFO) and its biodiesel (BPFO).

The characteristic absorption peaks of *Podocarpus falcatus* oil have been shown in Figure 7 in black. The absorption peak appearing at 722 cm^{-1} corresponds to the strain vibration of $-\text{CH}_2$, and the one at $1,744\text{ cm}^{-1}$ corresponds to the stretch vibration of the $\text{C}=\text{O}$ ester group. The spectrum of biodiesel shows an absorption peak appearing at $1,435\text{ cm}^{-1}$, characteristic of a methyl ester group ($\text{CO}-\text{O}-\text{CH}_3$), and the absorption peak at $1,194\text{ cm}^{-1}$ corresponding to the ester group (CO). The reduction in the peak at $1,435\text{ cm}^{-1}$ on the biodiesel spectrum can be attributed to the departure of the glycerol molecule and the appearance of CH_3-O vibrations in the biodiesel. Additionally, the separation of $1,169\text{ cm}^{-1}$ in the oil sample to $1,194\text{ cm}^{-1}$ and $1,171\text{ cm}^{-1}$ in the biodiesel sample indicates the conversion of the oil into biodiesel. Table 7 shows the characteristic band positions of the TF-IR for *Podocarpus falcatus* oil and the *Podocarpus falcatus* oil biodiesel produced.

3.5. UV-VIS Spectrophotometric Analysis of Oil and Biodiesel. Figure 8 below shows the superimposed UV-VIS spectra of *Podocarpus falcatus* oil and its biodiesel. In this figure, we observe an intense band around 250 nm on the

spectrum of *Podocarpus falcatus* oil which is not present on the spectrum of biodiesel. This peak observed at around 250 nm is probably absorption due to the $\pi \rightarrow \pi^*$ transition of the carbonyl of the triglycerides. A second peak is also observed around 300 nm which can be attributed to the $n \rightarrow \pi^*$ transition of the carbonyl. Moreover, from these curves, we can conclude that the absence of the $\pi \rightarrow \pi^*$ carbonyl transition of the triglycerides on the black spectrum confirms the absence of glycerol in the ester mixture formed.

4. Conclusions

Oil from *Podocarpus falcatus* was used to produce biodiesel by transesterification. The oil used was extracted mechanically using a hydraulic press that gave an extraction yield of 47.8% by mass, making the oil a promising raw material for the synthesis of biodiesel. Since an analysis of the oil showed that it had an acid number of less than 2%, the biodiesel was therefore produced through a one-step transesterification process with methanol, using KOH as catalyst. The optimization of the process was achieved by applying the response surface methodology, using the Box-Benhken design. The optimum conditions to produce the highest yield of biodiesel (96.1%) were as follows: a molar ratio of 10:1, a temperature of 50°C , and a reaction time of 180 minutes. The minimum viscosity, $3.58\text{ mm}^2/\text{s}$, was obtained at a molar ratio of 10:1, temperature of 50°C , and a duration of 120 min. Physicochemical analyses of both oil and the biodiesel using IR and UV-VIS confirmed the conversion of triglycerides into methyl esters, and that the properties of the biofuel produced comply with the standard prescribed by ASTM6751. Based on the results of this study, we can conclude that *Podocarpus falcatus* oil can be used as a non-edible oil to produce good quality biodiesel under optimal conditions.

Abbreviations

ANOVA: Analysis of variance
 ASTM: American Standard for Testing Materials
 BBD: Box-Benhken design
 BPFO: Biodiesel of *Podocarpus falcatus* oil

RSM: Response surface methodology
 FFA: Free fatty acid
 FT-IR: Fourier transform infrared spectroscopy
 PFO: Podocarpus falcatus oil
 UV-VIS: Ultraviolet-visible.

Data Availability

The numerical data used to support the findings of this study have been deposited in the Mendeley repository (doi:10.17632/2n5wst4r9x.1) or <https://data.mendeley.com/datasets/2n5wst4r9x/1/>.

Conflicts of Interest

The authors declare that they have no conflicts of interest.

Acknowledgments

The authors thank the assistance offered by NGUEDAP Richard of the University of Douala for the determination of the viscosity of the samples and all the members of the Research Unit/RU-NOGEE of the University of Dschang for their various contributions in the improvement of the quality of work. The authors would like to thank everyone who supported this study.

References

- [1] I. S. Manaf, N. H. Embong, S. N. M. Khazaai et al., "A review for key challenges of the development of biodiesel industry," *Energy Conversion and Management*, vol. 185, no. 10, pp. 508–517, 2019.
- [2] M. Ashjari, M. Garmroodi, F. A. Asl et al., "Application of multi-component reaction for covalent immobilization of two lipases on aldehyde-functionalized magnetic nanoparticles; production of biodiesel from waste cooking oil," *Process Biochemistry*, vol. 90, pp. 156–167, 2020.
- [3] R. Naveenkumar and G. Baskar, "Optimization and techno-economic analysis of biodiesel production from *Calophyllum inophyllum* oil using heterogeneous nanocatalyst," *Bioresource Technology*, vol. 315, no. 1, article 123852, 2020.
- [4] T. S. Singh and T. N. Verma, "Taguchi design approach for extraction of methyl ester from waste cooking oil using synthesized CaO as heterogeneous catalyst: response surface methodology optimization," *Energy Conversion and Management*, vol. 182, pp. 383–397, 2019.
- [5] H. Hosseinzadeh-Bandbafha, M. Tabatabaei, M. Aghbashlo, M. Khanali, and A. Demirbas, "A comprehensive review on the environmental impacts of diesel/biodiesel additives," *Energy Conversion and Management*, vol. 174, pp. 579–614, 2018.
- [6] A. Srivastava and R. Prasad, "Triglycerides-based diesel fuels," *Renewable and Sustainable Energy Reviews*, vol. 4, no. 2, pp. 111–133, 2000.
- [7] A. Kumar and S. Sharma, "Potential non-edible oil resources as biodiesel feedstock: an Indian perspective," *Renewable and Sustainable Energy Reviews*, vol. 15, no. 4, pp. 1791–1800, 2011.
- [8] T. Saba, J. Estephane, B. El Khoury et al., "Biodiesel production from refined sunflower vegetable oil over KOH/ZSM5 catalysts," *Renewable Energy*, vol. 90, no. 7, pp. 301–306, 2016.
- [9] R. Sakthivel, K. Ramesh, R. Purnachandran, and P. M. Shameer, "A review on the properties, performance and emission aspects of the third generation biodiesels," *Renewable and Sustainable Energy Reviews*, vol. 82, no. 3, pp. 2970–2992, 2018.
- [10] V. Singh, F. Bux, and Y. C. Sharma, "A low cost one pot synthesis of biodiesel from waste frying oil (WFO) using a novel material, β -potassium dizirconate (β -K₂Zr₂O₅)," *Applied Energy*, vol. 172, pp. 23–33, 2016.
- [11] A. Atabani, A. Silitonga, I. A. Badruddin, T. Mahlia, H. Masjuki, and S. Mekhilef, "A comprehensive review on biodiesel as an alternative energy resource and its characteristics," *Renewable and Sustainable Energy Reviews*, vol. 16, no. 4, pp. 2070–2093, 2012.
- [12] S. T. Keera, S. M. El Sabagh, and A. R. Taman, "Castor oil biodiesel production and optimization," *Egyptian Journal of Petroleum*, vol. 27, no. 4, pp. 979–984, 2018.
- [13] L. K. Sinha, S. Haldar, and G. C. Majumdar, "Effect of operating parameters on mechanical expression of solvent-soaked soybean-grits," *Journal of Food Science and Technology*, vol. 52, no. 5, pp. 2942–2949, 2015.
- [14] A. B. Fadhil and A. I. Ahmed, "Production of mixed methyl/ethyl esters from waste fish oil through transesterification with mixed methanol/ethanol system," *Chemical Engineering Communications*, vol. 205, no. 9, pp. 1157–1166, 2018.
- [15] S. Feleke, S. Haile, A. Alemu, and S. Abebe, "Characteristics of speed kernel oil from *Podocarpus falcatus*," *Journal of Tropical Forest Science*, vol. 24, no. 4, pp. 512–516, 2012.
- [16] R. A. Carr, "Refining and degumming systems for edible fats and oils," *Journal of the American Oil Chemists' Society*, vol. 55, no. 11, pp. 765–771, 1978.
- [17] M. M. Hassan and A. B. Fadhil, "Development of an effective solid base catalyst from potassium-based chicken bone (K-CBs) composite for biodiesel production from a mixture of non-edible feedstocks," *Energy Sources, Part A: Recovery, Utilization, and Environmental Effects*, vol. 43, pp. 1–16, 2021.
- [18] G. Dwivedi and M. P. Sharma, "Impact of cold flow properties of biodiesel on engine performance," *Renewable and Sustainable Energy Reviews*, vol. 31, pp. 650–656, 2014.
- [19] J. Gupta, M. Agarwal, and A. K. Dalai, "Optimization of biodiesel production from mixture of edible and nonedible vegetable oils," *Biocatalysis and Agricultural Biotechnology*, vol. 8, no. 1, pp. 112–120, 2016.
- [20] Z. Zhang and H. Zheng, "Optimization for decolorization of azo dye acid green 20 by ultrasound and H₂O₂ using response surface methodology," *Journal of Hazardous Materials*, vol. 172, no. 2-3, pp. 1388–1393, 2009.
- [21] P. Qiu, M. Cui, K. Kang et al., "Application of Box-Behnken design with response surface methodology for modeling and optimizing ultrasonic oxidation of arsenite with H₂O₂," *Open Chemistry*, vol. 12, no. 2, pp. 164–172, 2014.
- [22] G. Yin and Y. Dang, "Optimization of extraction technology of the *Lycium barbarum* polysaccharides by Box-Behnken statistical design," *Carbohydrate Polymers*, vol. 74, no. 3, pp. 603–610, 2008.
- [23] N. Aslan and Y. Cebeci, "Application of Box-Behnken design and response surface methodology for modeling of some Turkish coals," *Fuel*, vol. 86, no. 1-2, pp. 90–97, 2007.

- [24] K. Yetilmezsoy, S. Demirel, and R. J. Vanderbei, "Response surface modeling of Pb(II) removal from aqueous solution by *Pistacia vera* L.: Box -Behnken experimental design," *Journal of Hazardous Materials*, vol. 171, no. 1-3, pp. 551-562, 2009.
- [25] F. T. T. Rufis, I. Ionel, and S. G. Anagho, "A.C. Mihaiuti Optimization of the activated carbon preparation from avocado seeds, using the response surface methodology," *Revista de Chimie*, vol. 70, no. 2, pp. 410-416, 2019.
- [26] K. Krisnangkura, "A simple method for estimation of cetane index of vegetable oil methyl esters," *Journal of the American Oil Chemists Society*, vol. 63, no. 4, pp. 552-553, 1986.
- [27] A. Demirbas, "Biodiesel fuels from vegetable oils via catalytic and non-catalytic supercritical alcohol transesterifications and other methods: a survey," *Energy Conversion and Management*, vol. 44, no. 13, pp. 2093-2109, 2003.
- [28] K. Khiari, *Contribution à l'étude des propriétés thermophysiques des biocarburants de seconde génération et leur influence sur le comportement des moteurs*, Thèse de Doctorat/PhD, Ecole des Mines de Nantes, Nantes, France, 2016.
- [29] A. N. Sarve, M. N. Varma, and S. S. Sonawane, "Response surface optimization and artificial neural network modeling of biodiesel production from crude mahua (*Madhuca indica*) oil under supercritical ethanol conditions using CO₂ as co-solvent," *RSC Advances*, vol. 5, no. 85, pp. 69702-69713, 2015.
- [30] C. Senthilkumar, C. Krishnaraj, P. Sivakumar, and A. Sircar, "Statistical optimization and kinetic study on biodiesel production from a potential non-edible bio-oil of wild radish," *Chemical Engineering Communications*, vol. 206, no. 7, pp. 909-918, 2019.
- [31] U. C. F. Chigozie, A. Nnuekwe, O. Onukwuli, S. Ofochebe, and C. Ezekannagha, "Optimal route for effective conversion of rubber seed oil to biodiesel with desired key fuel properties," *Journal of Cleaner Production*, vol. 280, article 124563, 2021.
- [32] A. B. Fadhil, "Optimization of transesterification parameters of melon seed oil," *International Journal of Green Energy*, vol. 10, no. 7, pp. 763-774, 2013.
- [33] A. B. Fadhil, "Biodiesel production from beef tallow using alkali-catalyzed transesterification," *Arabian Journal for Science and Engineering*, vol. 38, no. 1, pp. 41-47, 2013.
- [34] C. Esonye, O. D. Onukwuli, and A. U. Ofoefule, "Optimization of methyl ester production from *Prunus Amygdalus* seed oil using response surface methodology and Artificial Neural Networks," *Renewable Energy*, vol. 130, pp. 61-72, 2019.
- [35] A. A. Ayola, F. K. Hymore, M. A. Obande, and I. Udeh, "Optimization of experimental conditions for biodiesel production," *International Journal Engineering and Technology*, vol. 12, no. 6, pp. 130-133, 2012.
- [36] K. Yamane, A. Ueta, and Y. Shimamoto, "Influence of physical and chemical properties of biodiesel fuels on injection, combustion and exhaust emission characteristics in a direct injection compression ignition engine," *International Journal of Engine Research*, vol. 2, no. 4, pp. 249-261, 2001.
- [37] D. R. T. Tchuifon, S. B. L. Ngomade, G. N. Ndifor-Angwafor et al., "Production of biodiesel by transesterification reaction of waste cooking oil," *Chemical Science International Journal*, vol. 3, no. 4, 2020.
- [38] M. Ahmad, S. Rashid, M. A. Khan, M. Zafar, S. Sultana, and S. Gulzar, "Optimization of base catalyzed transesterification of peanut oil biodiesel," *African Journal of Biotechnology*, vol. 8, no. 3, pp. 441-446, 2009.
- [39] B. K. Barnwal and M. P. Sharma, "Prospects of biodiesel production from vegetable oils in India," *Renewable and Sustainable Energy Reviews*, vol. 9, no. 4, pp. 363-378, 2005.
- [40] G. B. Adebayo, O. M. Ameen, and L. T. Abass, "Physico-chemical properties of biodiesel produced from *Jatropha curcas* oil and fossil diesel," *Journal of Microbiology and Biotechnology Research*, vol. 1, no. 1, pp. 12-16, 2011.
- [41] A. B. Fadhil, O. M. Nayyef, and S. H. Sedeeq, "Valorization of mixed radish seed oil and *Prunus armeniaca* L. oil as a promising feedstock for biodiesel production: evaluation and analysis of biodiesels," *Asia-Pacific Journal of Chemical Engineering*, vol. 15, no. 1, p. 2390, 2020.
- [42] A. B. Fadhil, S. H. Sedeeq, and N. M. Al-Layla, "Transesterification of non-edible seed oil for biodiesel production: characterization and analysis of biodiesel," *Energy Sources, Part A: Recovery, Utilization, and Environmental Effects*, vol. 41, no. 7, pp. 892-901, 2019.